

UC Irvine

UC Irvine Previously Published Works

Title

Aerosol chemical composition and distribution during the Pacific Exploratory Mission (PEM) Tropics

Permalink

<https://escholarship.org/uc/item/6pq9v1gd>

Journal

Journal of Geophysical Research, 104(D5)

ISSN

0148-0227

Authors

Dibb, JE
Talbot, RW
Scheuer, EM
[et al.](#)

Publication Date

1999-03-20

DOI

10.1029/1998jd100001

Copyright Information

This work is made available under the terms of a Creative Commons Attribution License, available at <https://creativecommons.org/licenses/by/4.0/>

Peer reviewed

Aerosol chemical composition and distribution during the Pacific Exploratory Mission (PEM) Tropics

J. E. Dibb,¹ R. W. Talbot,¹ E. M. Scheuer,¹ D. R. Blake,² N. J. Blake,² G. L. Gregory,³ G. W. Sachse,³ and D. C. Thornton⁴

Abstract. Distributions of aerosol-associated soluble ions over much of the South Pacific were determined by sampling from the NASA DC-8 as part of the Pacific Exploratory Mission (PEM) Tropics campaign. The mixing ratios of all ionic species were surprisingly low throughout the free troposphere (2–12 km), despite the pervasive influence from biomass burning plumes advecting over the South Pacific from the west during PEM-Tropics. At the same time, the specific activity of ⁷Be frequently exceeded 1000 fCi m⁻³ through much of the depth of the troposphere. These distributions indicate that the plumes must have been efficiently scavenged by precipitation (removing the soluble ions), but that the scavenging must have occurred far upwind of the DC-8 sampling regions (otherwise ⁷Be activities would also have been low). This inference is supported by large enhancements of HNO₃ and carboxylic acids in many of the plumes, as these soluble acidic gases would also be readily scavenged in any precipitation events. Decreasing mixing ratios of NH₄⁺ with altitude in all South Pacific regions sampled provide support for recent suggestions that oceanic emissions of NH₃ constitute a significant source far from continents. Our sampling below 2 km reaffirms the latitudinal pattern in the methylsulfonate/non-sea-salt sulfate (MSA/nss SO₄⁻) molar ratio established through surface-based and shipboard sampling, with values increasing from <0.05 in the tropics to nearly 0.6 at 70°S. However, we also found very high values of this ratio (0.2–0.5) at 10 km altitude above the intertropical convergence zone near 10°N. It appears that wet convective pumping of dimethylsulfide from the tropical marine boundary layer is responsible for the high values of the MSA/nss SO₄⁻ ratio in the tropical upper troposphere. This finding complicates use of this ratio to infer the zonal origin of biogenic S transported long distances.

1. Introduction

In September/October 1996 the NASA Global Tropospheric Experiment (GTE) mounted a two-aircraft airborne sampling campaign over a large expanse of the South Pacific Ocean. The primary objectives of the Pacific Exploratory Mission-Tropics (PEM-Tropics) were to test current understanding of nitrogen oxide/ozone chemistry by extensive sampling in a region where the levels of NO_x and O₃ (and most other tropospheric trace gases) were expected to be quite low, and to further understanding of sulfur cycling in and between the marine boundary layer and the free troposphere over the South Pacific where anthropogenic influences on the sulfur cycle should be small.

Each of the aircraft (the Wallops P3-B and the Ames DC-8) carried an extensive suite of instrumentation to measure the mixing ratios of various trace gases central to O₃ photochemical cycling and the S cycle, as well as to characterize the physical and chemical characteristics of aerosols. The scientific payloads of the planes

differed in some respects, reflecting the performance characteristics of the two platforms. The higher ceiling and greater range of the DC-8 make it better suited for surveys over large areas, while the low-altitude capabilities of the P3-B allow more detailed investigation of structure and processes within the marine boundary layer. The PEM-Tropics overview paper [Hoell *et al.*, this issue] provides details of the in situ and remote sensing instruments on both aircraft and describes the specific objectives of each mission flown during the deployment.

This paper is restricted to measurements made on the DC-8 and focuses on aerosol-associated soluble ionic species and the aerosol-associated cosmogenic radionuclide ⁷Be. Comparisons are made with the distributions of several trace gases also measured on the DC-8, and with the distributions of aerosol-associated species over the North Pacific measured in the first two GTE Pacific Exploratory Missions, PEM-West A and B.

2. Methods

2.1. Sampling

Aerosol samples were collected from the NASA DC-8 on 17 flights over the Pacific Ocean as part of the GTE PEM-Tropics mission in September–October 1996. We employed the same dual-inlet aerosol sampling system that was used on the GTE PEM-West missions [Dibb *et al.*, 1996, 1997]. One of the inlets was used to expose 2 μm pore size teflon (Gelman Zefluor) filters for the determination of the mixing ratios of soluble ionic species. The other inlet was generally used with glass fiber filters (Whatman GF/A) that were analyzed for the activities of the natural radionuclide tracers ⁷Be

¹Institute for the Study of Earth, Oceans, and Space, University of New Hampshire, Durham.

²Department of Chemistry, University of California, Irvine.

³NASA Langley Research Center, Hampton, Virginia.

⁴Department of Chemistry, Drexel University, Philadelphia, Pennsylvania.

Copyright 1999 by the American Geophysical Union.

Paper number 1998JD100001.
0148-0227/99/1998JD100001\$09.00

and ^{210}Pb . When samples for determination of the radionuclides were collected, the integration intervals of both systems were identical, so that the mixing ratios of the ionic species and the radionuclides were determined in the same air masses. Sampling for the radionuclides was interrupted when the DC-8 crossed the Intertropical and South Pacific convergence zones (ITCZ and SPCZ) to allow collection of large-volume samples for elemental analyses (by instrumental neutron activation), primarily for halogen species such as I. The results of these analyses are not discussed herein, but it is important to note that this modification to our usual sampling protocol resulted in collection of 40 samples for determination of ionic species mixing ratios without the radionuclide tracers.

Aerosol collection was restricted to flight legs at constant altitude. Exposure times in the mid and upper troposphere were usually in the 15–20 min range; below 2 km the integration interval was shortened to 10 min or less. A total of 322 samples was collected for ionic species analyses, with parallel samples for the radionuclide tracers in 282 of these intervals.

2.2 Analysis

Our analytical techniques were essentially unchanged from those used on the PEM-West campaigns [Dibb *et al.*, 1996, 1997]. However, we have slightly modified our handling of aerosol filters between exposure and analysis. On all GTE missions through PEM-West B our protocol involved placing exposed filters, still in the cassette, immediately into clean room bags and heat sealing them. Samples were then placed in a cooler with eutectic packs at -20°C for storage until extraction after the flight. Recognizing that the sealed bags contained a small amount of cabin air which could interact with the particles on the filter, we have begun including a purge of the bags with dry zero air. This procedure consists of sealing the clean bags with a tube delivering the zero air inside. A flow rate of about 2 L min^{-1} sweeps cabin air out of the bag and begins to inflate it. At this point the tube is withdrawn, and the bag is sealed again. Filters are then stored in a cooler. We have used this protocol for the Subsonic Assessment (SASS), Subsonic Aircraft Contrail and Cloud Effects Special Study (SUCCESS), and Subsonic Assessment Ozone and Nitrogen Oxide Experiment (SONEX) campaigns as well as during PEM-Tropics. The primary motivation for this change is to exclude any NH_3 in cabin air from contact with the exposed filters.

Concentrations of Cl^- , NO_3^- , SO_4^{2-} , $\text{C}_2\text{O}_4^{2-}$, CH_3SO_3^- , Na^+ , NH_4^+ , K^+ , Mg^{2+} , and Ca^{2+} in aqueous extracts of the teflon filters were determined by ion chromatography. Extractions and quantitation of the anionic species were conducted in the field within 24 hours of each flight. Aliquots of extracts were preserved with chloroform and returned to our laboratory in New Hampshire for cation determinations; these were completed within 6 weeks of the final flight. Glass fiber filters were express-mailed to New Hampshire at intervals through the campaign so that ^{7}Be activities could be determined by gamma spectrometry as quickly as possible. However, the large number of relatively small volume samples collected created a backlog, so the final filters were not counted until 2 months after the last flight. Our ^{210}Pb technique (determination of the activity of the ^{210}Po daughter by alpha spectrometry) requires approximately 1 year for in-growth of the daughter before counting [Dibb *et al.*, 1996]. At the time of writing, these analyses were in progress, with samples from the first 12 flights (approximately 1/2 of the total) completed. As a result, the ^{210}Pb distribution during PEM-Tropics will be presented in a subsequent paper.

2.3 Data Binning

The DC-8 flights during PEM-Tropics extended over a very large region, covering over 100° of longitude (108°W – 152°E) and extending from 55°N to 72°S (see overview paper by Hoell *et al.* [this issue]). In

order to organize discussion of our results, the samples were binned into seven regions and three altitude ranges. The vertical bins roughly correspond to the marine boundary layer ($<2\text{ km}$), the lower to midtroposphere (2–8 km), and the upper troposphere ($>8\text{ km}$). The highest bin includes a few penetrations of the lower stratosphere in the higher-latitude spatial regions ($>15^\circ\text{N}$ and $>35^\circ\text{S}$)

Selection of regional bins was based on a combination of large-scale features of atmospheric circulation convolved with the DC-8 flight tracks. In the northern hemisphere we defined two latitude bands ($>15^\circ\text{N}$ and 0° – 15°N) on the basis of the position of the Intertropical Convergence Zone (ITCZ). Two latitude belts were defined in the southern hemisphere; a tropical and subtropical band (0° – 35°S) and mid to high latitudes ($>35^\circ\text{S}$). The operational bases of the DC-8 suggested three longitudinal zones, with flights out of Fiji and New Zealand defining the western region (west of 170°W), those out of Hawaii and Tahiti sampling the central zone (120°W to 170°W), and the Easter Island flights defining the eastern region (east of 120°W). See Figure 1 and its caption for a graphical representation of the regional bins.

The South Pacific Convergence Zone (SPCZ) represents another possible meteorological dividing line within our 0° – 35°S latitude band. Gregory *et al.* [this issue] document and discuss the large spatial gradients in the mixing ratios of many species across the SPCZ. The aerosol-associated species that are the focus of this paper showed little difference on opposite sides of the SPCZ. We also considered dividing this bin at 15°S to reflect the oceanographic boundaries between the south equatorial current and the subtropical gyre. This division reveals nearly two-fold higher sea-salt concentrations in the boundary layer 15° – 35°S compared to 0° – 15°S in the western most region, a smaller boundary layer enhancement of sea-salt in the southerly portion of the central region, but no significant differences for the other species, or at higher altitudes. We therefore chose to maintain the 0° – 35°S region as three bins rather than six with smaller numbers of samples in each.

In several sections of this paper we make comparisons between the aerosol composition and the mixing ratios of various trace gases measured by other experimenters on the DC-8. The sampling frequencies for analysis of these other species were all shorter than our integration intervals, but were not always the same for different gaseous species. We use a merged data file (generated at Harvard University) wherein the mixing ratios of all other parameters measured from the DC-8 were averaged over the aerosol sampling times to make these comparisons. This and several other merged products, as well as the original data reported from all instruments, are archived in the Langley Distributed Active Archive Center (DAAC).

3. Results

Aerosol composition in the 21 space-height bins described above is statistically summarized in Table 1. It should be noted that the mixing ratios of one or more of the species of interest were often below our detection limit. The detection limits are largely determined by variability in the concentrations of the analytes extracted from blank filters (which were generated at a rate of at least 2/flight by loading a filter into the sampling system, opening all valves to allow airflow for 15 s, and then removing the filter). We subtract the mission specific mean blank ($\text{nmol of analyte filter}^{-1}$) from each sample. Therefore the mixing ratios at detection limit vary inversely with the volume of air filtered for each sample. During PEM-Tropics our mean (standard deviation) blank values were 4.1 (2.8), 9.5 (7.5), 1.9 (1.8), 0.7 (1.9), 0.02 (0.08), 25.7 (16.2), 7.1 (4.5), 6.6 (5.2), 3.3 (1.3), and 1.2 (0.6) nmol filter^{-1} of Cl^- , NO_3^- , SO_4^{2-} , $\text{C}_2\text{O}_4^{2-}$, CH_3SO_3^- , Na^+ , NH_4^+ , K^+ , Ca^{2+} , and Mg^{2+} , respectively. Sample volumes ranged from 0.8–16.6 $\text{m}^3\text{ STP}$, with mean and median values of 4.2 and 3.8, respectively. For a

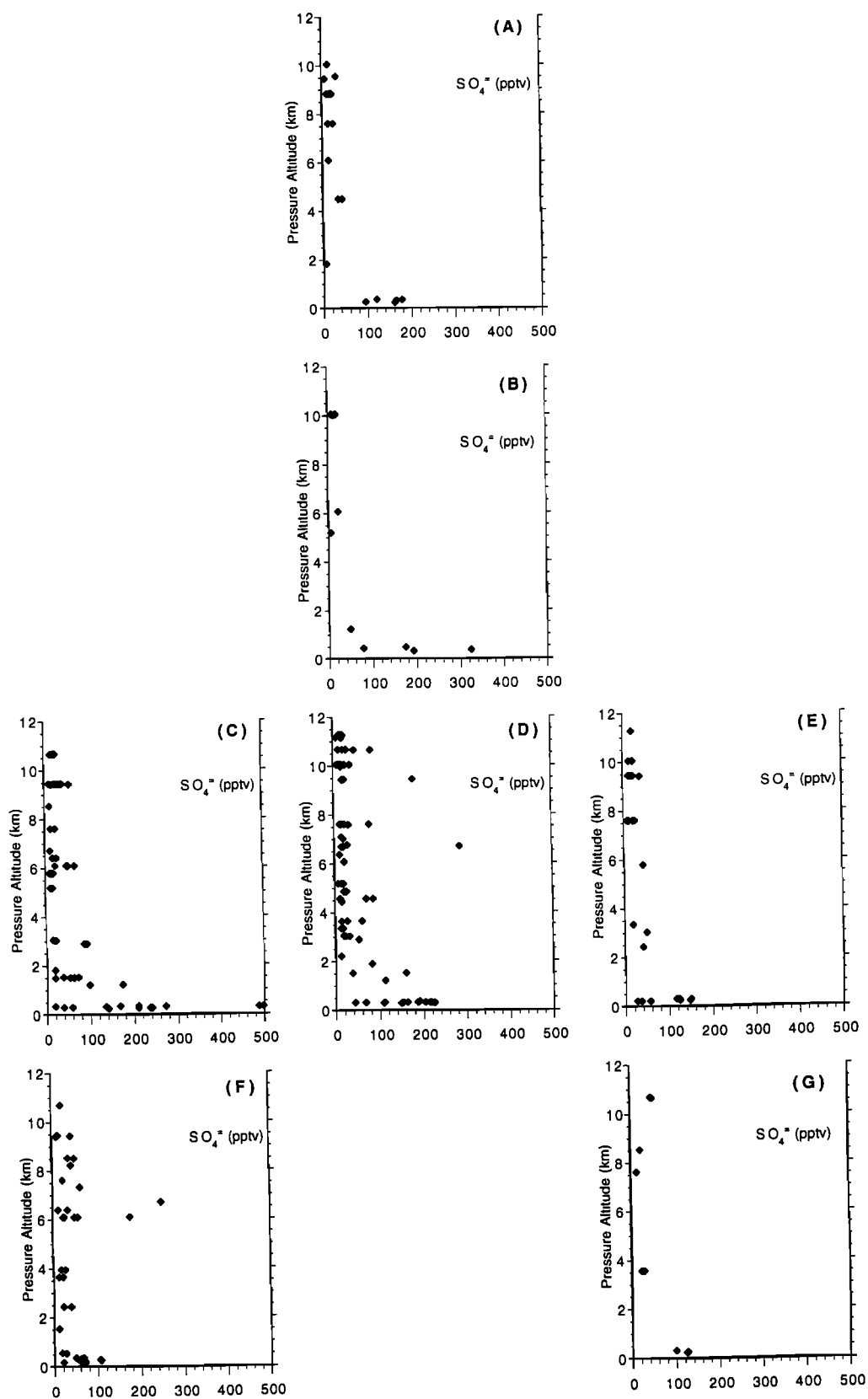


Figure 1. Altitude distribution of aerosol-associated $\text{SO}_4^=$ in the seven geographic regions sampled from the DC-8 during PEM-Tropics. The regions are the same as those defined in Table 1: (a) $>15^\circ\text{N}$, $120^\circ\text{-}170^\circ\text{W}$, (b) $0^\circ\text{-}15^\circ\text{N}$, $120^\circ\text{-}170^\circ\text{W}$, (c) $0^\circ\text{-}35^\circ\text{S}$, West of 170°W , (d) $0^\circ\text{-}35^\circ\text{S}$, $120^\circ\text{-}170^\circ\text{W}$, (e) $0^\circ\text{-}35^\circ\text{S}$, East of 120°W , (f) $>35^\circ\text{S}$, West of 170°W , (g) $>35^\circ\text{S}$, East of 120°W .

Table 1. Summary of Aerosol Composition, Binned by Region and Altitude

	Cl ⁻	NO ₃ ⁻	SO ₄ ²⁻	C ₂ O ₄ ²⁻	MSA	Na ⁺	NH ₄ ⁺	K ⁺	Ca ²⁺	Mg ²⁺	⁷ Be
<i>>15°N, 120°-170°W</i>											
					<i>0-2 km</i>		<i>Six Samples^a (6)</i>				
Mean	533	28	120	1.6	8.1	1025	122	73	40	119	382
s.d.	740	16	64	0.4	6.8	824	126	23	21	98	
Median	130	28	140	1.6	11.0	1316	82	73	52	152	
<i>n</i>	3	4	6	2	3	5	6	2	3	5	1
<i>2-8 km</i> <i>Seven Samples^a (7)</i>											
Mean	25	67	26			30	62	10	21	7	245
s.d.	--	37	13			--	33	--	14	--	111
Median	25	67	25			30	64	10	21	7	243
<i>n</i>	1	2	5	0	0	1	6	1	2	1	6
<i>>8 km</i> <i>12 Samples^a (12)</i>											
Mean		13	17				59				986
s.d.		5	8				19				1069
Median		15	17				59				530
<i>n</i>	0	3	7	0	0	0	5	0	0	0	9
<i>0°-15°N, 120°-170°W</i>											
					<i>0-2 km</i>		<i>Five Samples^a (2)</i>				
Mean	1112	29	163	1.9	1.0	961	186	19	46	114	
s.d.	921	24	109	--	--	623	111	8	28	77	
Median	1064	24	174	1.9	1.0	1122	159	19	33	132	
<i>n</i>	5	5	5	1	1	5	5	2	3	5	0
<i>2-8 km</i> <i>Five Samples^a (0)</i>											
Mean	89	19	14				22		20	7	
s.d.	71	17	12				--		--	--	
Median	89	16	14				22		20	7	
<i>n</i>	2	3	2	0	0	0	1	0	1	1	0
<i>>8 km</i> <i>Six Samples^a (1)</i>											
Mean	23	68	13		3.5		69		17		
s.d.	4	23	5		1.4		34		4		
Median	23	68	13		3.7		62		17		
<i>n</i>	2	2	5	0	5	0	5	0	2	0	0
<i>0°-35°S, East of 120°W</i>											
					<i>0-2 km</i>		<i>Eight Samples^a (8)</i>				
Mean	996	46	97		2.3	993	123	43	31	113	
s.d.	763	23	50		1.0	706	46	24	7	81	
Median	1088	45	119		2.0	1094	129	35	35	134	
<i>n</i>	8	5	8	0	8	8	8	5	5	8	0
<i>2-8 km</i> <i>Twelve Samples^a (12)</i>											
Mean	47	24	24		0.7	47	61	17		9	582
s.d.	21	20	15		--	55	25	--		--	270
Median	47	22	20		0.7	47	46	17		9	604
<i>n</i>	2	7	10	0	1	3	11	1	0	1	9
<i>>8 km</i> <i>10 Samples^a (10)</i>											
Mean	33	35	21	3		84	43	20			539
s.d.	--	9	9	--		--	24	--			302
Median	33	35	20	3		84	40	20			439
<i>n</i>	1	2	7	1	0	1	8	1	0	0	8
<i>0°-35°S, 120°-170°W</i>											
					<i>0-2 km</i>		<i>18 Samples^a (18)</i>				
Mean	1127	77	136	1.7	1.3	957	159	43	44	88	203
s.d.	731	102	64	--	0.8	718	78	20	39	61	76
Median	1116	47	150	1.7	1.2	885	163	45	34	69	179
<i>n</i>	18	17	18	1	14	16	17	9	13	17	12
<i>2-8 km</i> <i>46 Samples^a (45)</i>											
Mean	116	61	33	6.2	0.3	183	73	42	19	53	363
s.d.	234	46	44	4.5	0.0	308	89	39	5	56	287
Median	47	44	21	6.8	0.3	75	53	22	20	21	277
<i>n</i>	14	22	42	4	3	9	33	9	3	5	36
<i>>8 km</i> <i>40 Samples^a (40)</i>											
Mean	46	65	28	9.8	0.5	64	53	23	18	16	558
s.d.	19	76	34	9	0.0	--	57	10	2	--	439
Median	42	35	19	9.4	0.5	64	30	19	18	16	434
<i>n</i>	5	17	28	3	2	1	27	9	2	1	29
<i>0°-35°S, West of 170°W</i>											
					<i>0-2 km</i>		<i>22 Samples^a (12)</i>				
Mean	1111	62	154		1.4	1207	125	69	45	127	540
s.d.	991	42	138		1.1	856	78	32	24	95	0
Median	933	42	135		1	1133	102	68	47	112	540
<i>n</i>	19	11	21	0	16	19	22	12	12	18	2

Table 1. (continued)

	Cl ⁻	NO ₃ ⁻	SO ₄ ⁻	C ₂ O ₄ ⁻	MSA	Na ⁺	NH ₄ ⁺	K ⁺	Ca ²⁺	Mg ²⁺	⁷ Be
<i>2-8 km 36 Samples^a (31)</i>											
Mean	72	39	30		0.3	114	59	24	28	11	601
s.d.	92	30	25		0.1	88	30	10	14	6	467
Median	38	28	19		0.3	65	53	22	24	8	394
<i>n</i>	11	15	20	0	3	3	21	7	3	6	24
<i>>8 km 32 Samples^a (21)</i>											
Mean	41	41	26		0.8		112	19	23	8	775
s.d.	25	26	14		0.4		55	3	8	1	433
Median	27	35	25		1.0		81	19	23	8	686
<i>n</i>	7	6	14	0	3	0	8	3	2	2	13
<i>>35°S, East of 120°W 0-2 km Three Samples^a (3)</i>											
Mean	1638	31	116		1.1	1705	114	46	41	195	134
s.d.	391	16	15		0.2	410	28	21	12	34	0
Median	1551	31	123		1.1	1659	129	38	48	208	134
<i>n</i>	3	2	3	0	3	3	3	3	3	3	2
<i>2-8 km Three Samples^a (3)</i>											
Mean	51		21				99				467
s.d.	--		8				20				0
Median	51		22				105				467
<i>n</i>	1	0	3	0	0	0	3	0	0	0	2
<i>>8 km Four Samples^a (4)</i>											
Mean		13	36				119				4081
s.d.		--	8				64				3172
Median		13	36				134				3450
<i>n</i>	0	1	4	0	0	0	4	0	0	0	4
<i>>35°S, West of 170°W 0-2 km 15 Samples^a (15)</i>											
Mean	947	68	54	3.3	1.5	724	69	63	28	83	172
s.d.	993	31	32	1.5	1.2	692	63	49	19	75	36
Median	502	51	57	3.3	0.9	425	47	49	23	49	172
<i>n</i>	14	7	12	2	11	13	8	8	5	11	7
<i>2-8 km 23 Samples^a (23)</i>											
Mean	42	54	54			95	136	98	26	7	669
s.d.	30	39	65			--	158	49	--	--	522
Median	29	41	28			95	60	98	26	7	485
<i>n</i>	3	10	16	0	0	1	10	2	1	1	21
<i>>8 km Nine Samples^a (9)</i>											
Mean	65	30	29				51	16			1363
s.d.	47	4	17				24	--			1295
Median	65	30	29				41	16			688
<i>n</i>	2	2	8	0	0	0	4	1			9

Units are pptv for all species except ⁷Be, which is reported as fCi m⁻³ STP; *n* is the number of samples above our detection limits for the given species in each bin; s.d., standard deviation. See text for discussion of the precautions which should be taken when comparing these data to results from other campaigns.

^aThe number of samples collected for determination of soluble ion mixing ratios (followed by the number for radionuclide analyses) in each geographic/altitude bin.

sample of mean volume the standard deviation of the blanks leads to an uncertainty in mixing ratio of 15, 40, 10, 10, 0.4, 86, 24, 28, 7, and 3 pptv for the ions (listed in same order as above). These uncertainties decrease (increase) proportionately as the volume of air sampled increases (decreases).

Deciding how to incorporate samples below detection limits when calculating descriptive statistics is problematic. Considering such samples to be zeros would depress mean and median values artificially. Similarly, inserting the detection limit, or some constant fraction of it, could significantly overestimate the true mixing ratio, especially for small volume samples. We have calculated the summary statistics in Table 1 on the basis of those samples that were above detection limits, thus the means and medians often represent upper limit values. We also report the total number of samples collected, and those above detection limits for each species, in each of the bins.

We were able to quantify SO₄⁻, NH₄⁺, and ⁷Be in 76, 67, and 69%, respectively, of all samples collected (Table 1). All other species were below detection limits more often than not, with the percentage of samples above detection limits ranging from 4% (C₂O₄⁻) to 44% (NO₃⁻). Below 2 km we were able to determine mixing ratios of all species except C₂O₄⁻ most of the time, with K⁺ above detection least often (53% of samples) and SO₄⁻ nearly always quantified (95% of samples) (Table 1).

3.1. Spatial Distributions

3.1.1. Free troposphere. We focus first on the distributions of SO₄⁻, NH₄⁺, and ⁷Be, since our data set for these species allows examination of variations with height as well as between geographic regions. In most of the regional bins the mixing ratios of SO₄⁻ and NH₄⁺ tended to decrease rapidly with height, while ⁷Be increased (Figures 1-3). Below 2 km the range of SO₄⁻ and NH₄⁺ mixing ratios in most regions was substantial.

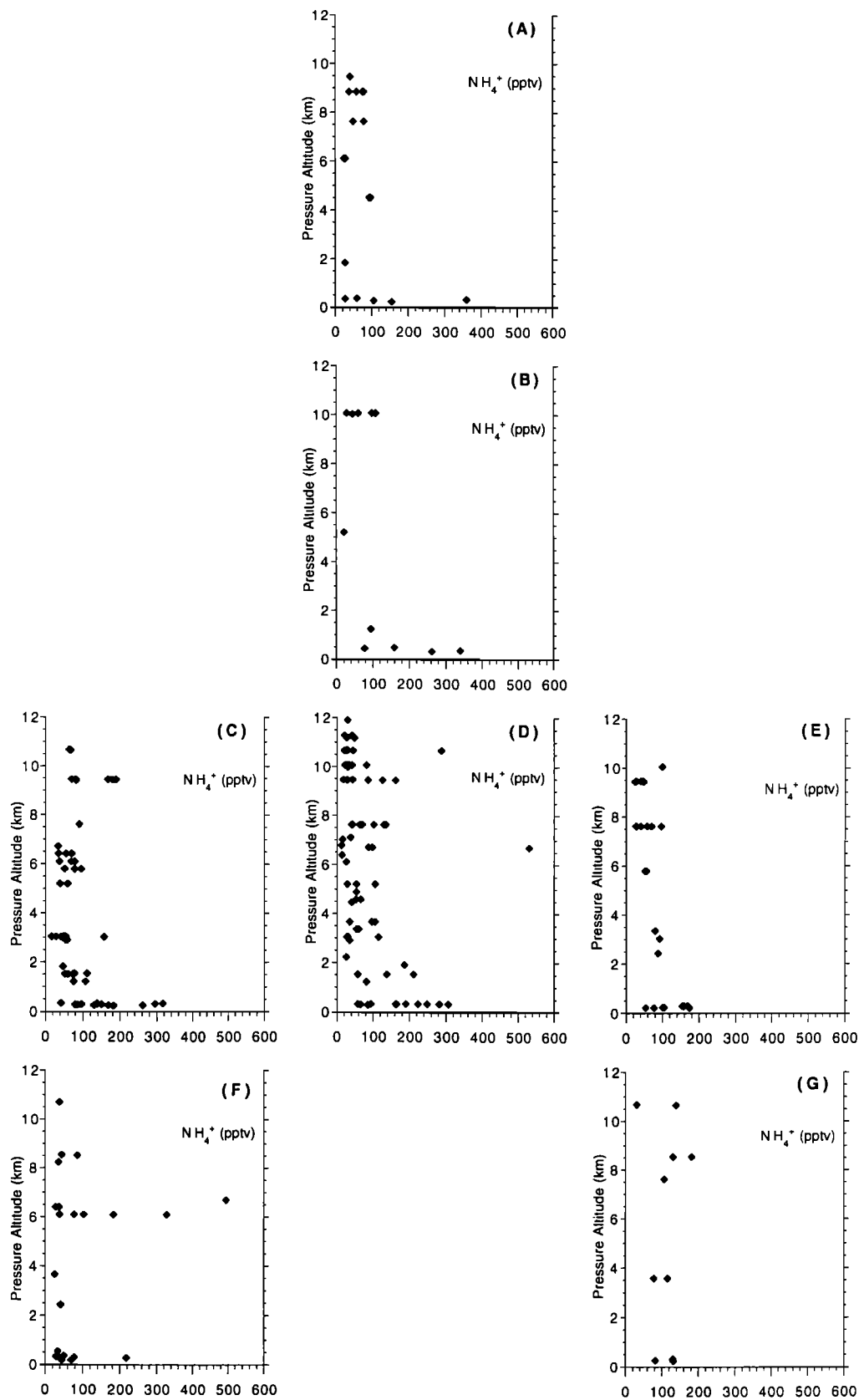


Figure 2. As in Figure 1, but for aerosol-associated NH_4^+ .

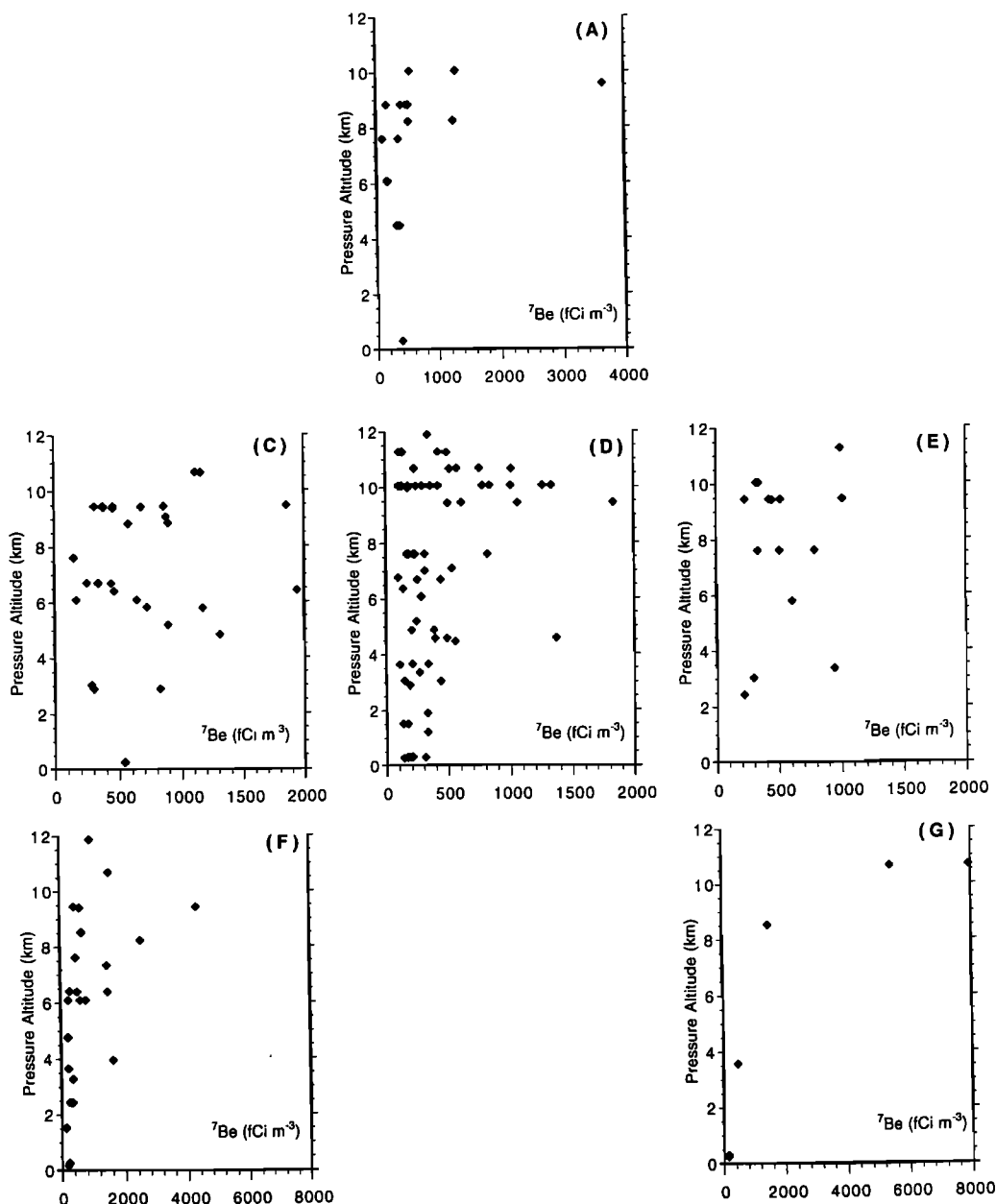


Figure 3. As in Figure 1, but for aerosol-associated ^7Be . Note that only three samples were collected for ^7Be determination in the region of Figure 1b, and they were all below detection limit. Also, note the changes in activity scale between the three latitude bands (greater range at higher latitudes).

There was a tendency for the greatest mixing ratios to occur at the lowest sampling altitude with substantially lower values often found only a few hundred meters higher (Figures 1 and 2). The small number of samples and large variability in the <2 km bins make differences between regions statistically insignificant, but the mean and median SO_4^- and NH_4^+ mixing ratios were highest in the 0° - 15°N region and lowest in the high southern latitude, western region (Table 1). In the middle troposphere (2-8 km) the situation was reversed, with the mixing ratios of both species quite low or below detection limits in the 0° - 15°N bin and the highest mean concentrations found at latitudes greater than 35°S in the western Pacific (Table 1). However, the elevated mean SO_4^- and NH_4^+ mixing ratios in this bin reflect several highly enriched samples (Figures 1 and 2). If medians are compared rather than means, the SO_4^- enhancement in the $>35^\circ\text{S}$, W bin was very modest, and the highest

NH_4^+ value was found in the eastern high-latitude 2-8 km bin instead (Table 1). At the highest sampling altitudes the mean and median SO_4^- mixing ratios were lowest north of the equator and highest south of 35°S , but nearly constant zonally within the two southern hemisphere latitude bands. In contrast, mean NH_4^+ mixing ratios increased from east to west in the 0° - 35°S band, but were higher in the eastern, compared to western, bin south of 35°S (Table 1).

Beryllium 7 was often below detection limit in the <2 km altitude range, so comparison of means and medians between all regions are not very informative. Between 2 and 8 km, mean and median ^7Be activities increased considerably relative to boundary layer values in each region (bearing in mind that the high values reported for the lowest altitude in the 0° - 15°N and 0° - 35°S western regions represent only 1 or 2 samples with detectible ^7Be , while 5 times as many samples were below

detection limits in each region) (Table 1 and Figure 3). Concentrations of ^{7}Be in the middle troposphere averaged 1.3–2.7 times higher in the four eastern and western regions compared to the regions between 120° and 170°W . It should also be noted that the ^{7}Be activity in the 2–8 km altitude range varied widely. In all regions where >3 samples were collected the standard deviation exceeded 45% of the mean and was $\geq 78\%$ of the mean in three of the five southern hemisphere regions (Table 1). Above 8 km, penetration of the lower stratosphere yielded high ($>>1000\text{ fCi m}^{-3}$) ^{7}Be activities in some samples from each of the high-latitude regions (Figure 3), causing average values to increase two- to eight-fold relative to the 2–8 km altitude range in these regions. Within the 0° – 35°S latitude band, mean and median ^{7}Be activities showed little difference between the 2–8 and >8 km altitude ranges (Table 1 and Figure 3), with the largest increase (in the central region) about a factor of 1.5.

3.1.2. Boundary layer. Sea salt constitutes the overwhelmingly dominant fraction of aerosols in the <2 km range in all regions sampled. We found a wide range in mixing ratios of all species derived from sea salt (e.g., Na^+ , Mg^{2+} , Ca^{2+} , and Cl^-) within each geographic bin (Table 1), but a large part of this variability is an artifact of our altitude binning. Steep gradients in the mixing ratios of sea-salt-derived species were often observed between the lowest sampling altitude of the DC-8 (approximately 0.3 km) and 2 km, similar to the vertical distributions of SO_4^{2-} and NH_4^+ shown in Figures 1 and 2. Furthermore, the abundance of sea-salt aerosol in the marine boundary layer varies rapidly in response to the wind field and as a result of precipitation scavenging. Since we have very little insight into the history of the marine boundary layer air masses in the hours to days before the DC-8 encountered them, our discussion of boundary layer aerosols will focus on spatial variations of species ratios rather than the abundance of individual species.

3.2. Comparison to Previous Measurements

Most measurements of aerosol composition in the South Pacific have been conducted at sea level sites, often on islands, or on board ship [e.g., Ayers *et al.*, 1986; Raemdonck *et al.*, 1986; Saltzman *et al.*, 1986a; Bates *et al.*, 1989, 1992a; Pszenny *et al.*, 1989; Savoie and Prospero, 1989; Yamato *et al.*, 1989; Quinn *et al.*, 1990; Clarke and Porter, 1993; Huebert *et al.*, 1993]. Sampling has therefore focused on the bottom few tens of meters of the marine boundary layer, a region that is not accessible by the DC-8 platform. We suspect that agreement between our measurements of mixing ratios in a given region and previous results from surface-based sampling would be fortuitous for the reasons outlined above. Thus we will not make comparisons of absolute abundance of individual species, but in the following discussion we do examine our observed spatial variations in key ratios of species in the context of the patterns documented through surface-based campaigns.

Airborne sampling of aerosols presents a number of serious challenges related to the possible failure of the nozzle, inlet, and tubing to pass a representative sample of the ambient aerosol population to the actual sampling device (a filter in our case) [e.g., Huebert *et al.*, 1990; Porter *et al.*, 1992]. Our approach to meeting these challenges is outlined by Dibb *et al.* [1996]. Previous airborne sampling campaigns that characterized the distribution of aerosol-associated species over the South Pacific (e.g., Global Atmospheric Measurements Experiment on Tropospheric Aerosols and Gases (GAMETAG), First Aerosol Characterization Experiment (ACE 1)) used different sampling systems on platforms with operational characteristics unlike those of the DC-8. Similarly, the aerosol composition measurements made from the P-3B during PEM-Tropics [Hoell *et al.*, this issue], while showing general agreement

with our results over large scales in the regions sampled by both aircraft (B. Heikes, personal communication, September 1997), may not be directly comparable in detail due to a combination of different sampling altitudes, spatial resolution, and the possibility that one or both systems suffer systematic sampling bias. In particular, we note that fast response instrumentation on both aircraft revealed large spatial gradients in CO , O_3 , and aerosol number distributions within the marine boundary layer. Such gradients would have made rigorous intercomparison flights difficult to execute and suggest that there is little assurance that the DC-8 and P-3B actually sampled the same boundary layer air masses during the loosely coordinated flights that were conducted during PEM-Tropics. We recognize that the issue of sampling artifacts is a pressing concern for all groups collecting aerosol samples from airborne platforms and careful intercomparisons are needed. However, it is not possible to establish equivalence or discrepancies between our system and those on other platforms from data presently available. Therefore our focus will be solely on measurements that we have made from the DC-8 over the past 5 years.

The dual-inlet aerosol sampling system we fly on the DC-8, and the filter extraction and analytical procedures, have remained essentially unchanged through the three GTE Pacific Exploratory Missions (PEM-West A, PEM-West B, and PEM-Tropics) (as well as the Sub-sonic Assessment (SASS) SUCCESS mission over the central United States in spring 1996 and the SONEX mission over the North Atlantic in fall 1997). Comparison of the aerosol distributions we found on the three PEM campaigns should reflect real differences in the composition of the atmosphere over the North and South Pacific, though there may also be some influence of seasonal [Dibb *et al.*, 1997] and/or secular changes over the 5 year period between PEM-West A and PEM-Tropics.

PEM-West A was conducted in September–October 1991 [Dibb *et al.*, 1996], while PEM-West B occurred in February–March 1994 [Dibb *et al.*, 1997], in order to document the seasonal variation in the magnitude of Asian outflow over the North Pacific. In both campaigns, flights were conducted out of Hong Kong and Yakota, Japan (termed near Asia), and from Guam and Hawaii (termed remote Pacific) (Table 2). As expected, mixing ratios of species with strong anthropogenic sources like SO_4^{2-} and NH_4^+ (plus a host of trace gases) and tracers of continental dust (non-sea-salt Ca^{2+} in our data set) were higher near Asia during both missions and increased between fall and spring in response to the climatological increase in the strength and persistence of westerly winds blowing from Asia over the western North Pacific [see Dibb *et al.*, 1997, and references therein]. (Calcium is not included in Table 2, since the mixing ratios of Ca^{2+} in all PEM-Tropics samples were consistent with a sea-salt source.) However, the Asian outflow signal in aerosol-associated ionic species in both seasons was restricted to the lower troposphere, with upper tropospheric air generally quite "clean" (Table 2). The activity of ^{7}Be (an aerosol-associated tracer of upper tropospheric and stratospheric origin) was also much lower than anticipated in the upper troposphere over the North Pacific. In contrast, insoluble gaseous tracers of industrial activity were elevated throughout the troposphere over much of the North Pacific. We concluded that the low mixing ratios of aerosol-associated species were due to extensive wet scavenging in deep convection that pumped continental boundary layer air from Asia into the mid and upper troposphere where it could be advected over the Pacific [Dibb *et al.*, 1996, 1997].

Mean mixing ratios of SO_4^{2-} in the boundary layer near Asia during both PEM-West missions were more than two-fold (up to nine-fold) greater than in any of the 0–2 km bins sampled during

Table 2. Mean Mixing Ratios of Selected Aerosol-Associated Species in the North Pacific During the GTE PEM-West Missions

Altitude Range, km	SO ₄ ²⁻ , pptv	NH ₄ ⁺ , pptv	Mg ²⁺ , pptv	⁷ Be, fCi m ⁻¹
<i>PEM-West A^a, Near Asia</i>				
0.3-1.8	364	487	59	89
2-7	58	146	13	231
7-8.5	30	47	6	181
8.5-12.5	25	55	29	143
<i>PEM-West A^a, Remote Pacific</i>				
0.3-1.8	233	335	68	69
2-7	25	28	12	137
7-8.5	31	35	22	74
8.5-12.5	18	36	--	176
<i>PEM-West B^b, Near Asia</i>				
<1	500	646	69	158
1-6	242	394	69	277
6-9	47	129	24	372
>9	126	55	10	3207
<i>PEM-West B^b, Remote Pacific</i>				
<1	174	239	22	125
1-6	51	79	16	66
6-9	12	22	17	125
>9	13	27	10	370

^aThe complete PEM-West A aerosol composition data set is presented by Dobb et al., [1996].

^bThe complete PEM-West B aerosol composition data set is presented by Dobb et al. [1997].

PEM-Tropics (Tables 1 and 2). This enhancement near Asia extended up into the lower troposphere during PEM-West B (compare the near Asia 1-6 km, or the mean of the 1-6 and 6-9 km, bins (Table 2) to all 2-8 km bins from PEM-Tropics (Table 1)). The remote North Pacific SO₄²⁻ mixing ratios were comparable to those in the South Pacific. The slight enhancement in the northern low-altitude bins is probably mainly due to the shallower bins used for these missions (Tables 1 and 2). Elevated SO₄²⁻ mixing ratios above 9 km near Asia during PEM-West B reflect stratospheric air encountered in a tropopause fold [Dobb et al., 1997]. If these samples are excluded, the mean SO₄²⁻ mixing ratios in all high-altitude bins during the three missions range from 13 to 36 parts per trillion by volume (pptv), with high and low values within this relatively narrow range occurring on both sides of the equator.

Comparing NH₄⁺ mixing ratios between the North and South Pacific also reveals the continental influence on the boundary layer near Asia, where levels were again 2-9 times higher than the average in any <2 km bin during PEM-Tropics. The remote North Pacific boundary layer bins during both PEM-West campaigns also had higher NH₄⁺ mixing ratios than any of the <2 km bins during PEM-Tropics including the two north of the equator (Tables 1 and 2). If, as we argue below, the ocean is a significant source of NH₃, part of this difference may be due to the 1 km top used for PEM-West boundary layer bins compared to 2 km for PEM-Tropics. In the low to middle troposphere the NH₄⁺ comparisons are mixed, with PEM-Tropics means exceeding those in the remote North Pacific, but the highest means were found near Asia. At the highest altitudes (above 8 or 9 km) the differences in NH₄⁺ mixing ratios are relatively small, except for the much higher averages in the PEM-Tropics western 0°-35°S and eastern high southern latitude regions (Tables 1 and 2). In the 0°-35°S bin this average is clearly an overestimate, since the NH₄⁺ mixing ratio was below detection limit in 75% of the samples, but in the eastern zone above 35°S, NH₄⁺ was quantified in all of the high-altitude samples.

Magnesium is included in Table 2 as an indicator of sea-salt aerosol, though a minor fraction of Mg²⁺ in the near Asia bins

during both PEM-West missions was likely of continental dust origin. All low-altitude PEM-Tropics bins had higher Mg²⁺ mixing ratios than any of the PEM-West regions, implying more sea-salt aerosol in the marine boundary layer. In the free troposphere bins the reverse is generally true, the sole exception being the high Mg²⁺ mixing ratio in the central 0°-35°S region of PEM-Tropics (Tables 1 and 2).

Beryllium 7 was often below detection limits in the boundary layer bins of all three missions, so the means reported in Tables 1 and 2 should be viewed with caution. In the free troposphere the mean ⁷Be activities were markedly higher in all of the PEM-Tropics regions. Perhaps of even greater relevance is the observation that below 8 km during both PEM-West missions the ⁷Be activity never exceeded 500, and was only rarely above 300, fCi m⁻³ [Dobb et al., 1996, 1997]. During PEM-Tropics ⁷Be activities >1000 fCi m⁻³ were measured throughout the troposphere in all of the southern hemisphere regions (Figure 3). In the highest-altitude range the high mean ⁷Be activities at latitudes above 15°N or 35°S during PEM-Tropics, and in the PEM-West B near Asia bin, reflect penetration of the stratosphere in several of the sample collection intervals. For those regions where the high-altitude bin was entirely within the troposphere, ⁷Be activities were also greater during PEM-Tropics by factors ranging from 1.5 to 5.5 (Tables 1 and 2).

4. Discussion

4.1. Tropospheric Distributions

4.1.1. Biomass burning plumes. During PEM-Tropics the troposphere in western and central regions of the South Pacific was heavily impacted by emissions from biomass burning. These emissions were manifested as huge "plumes" up to several kilometers thick with elevated mixing ratios of O₃, CO, PAN, nitric, and carboxylic acids, and a suite of nonmethane hydrocarbons [e.g., Talbot et al., this issue]. These plumes were all advected into the DC-8 sampling region from the west and had been over the South

Pacific for at least several days, and usually much longer, before we intercepted them [Fuelberg *et al.*, this issue].

Biomass burning plumes from boreal and tropical fires have been characterized in many previous investigations (e.g., the GTE Atmospheric Boundary Layer Experiment (ABLE 2), ABLE 3, and Transport and Atmospheric Chemistry Near the Equatorial Atlantic (TRACE A) campaigns, and Dynamique et Chimie Atmosphérique en Forêt Equatoriale (DECAFE)). Such plumes generally contain large enhancements in aerosol-associated species, most often including elemental C, NH_4^+ , and K^+ , though some have also had enhanced NO_3^- and SO_4^{2-} . In this light, the low mixing ratios of aerosol-associated soluble ions measured throughout the PEM-Tropics study area are noteworthy.

In the central and western South Pacific regions, biomass burning plumes were encountered on every flight, and nearly all of these were in the 2–8 km altitude range. We noted earlier that the mean mixing ratios of SO_4^{2-} and NH_4^+ were slightly higher in the western high-latitude midtroposphere than any other bin; but that these averages were pulled up by two samples with very high mixing ratios. Closer examination of Figures 1 and 2 reveals that the mixing ratios of SO_4^{2-} and NH_4^+ in the 2–8 km range in the three southern hemisphere regions west of 120°W were below 100 and 200 pptv, respectively, in all except three samples (one in the central region and two in the high-latitude western zone). These three samples were all collected on the transit flight from Tahiti to New Zealand (flight 12).

Two separate plumes were encountered on flight 12 (Figure 4). The first plume, just before 2200 UTC, is representative of nearly all plumes encountered during PEM-Tropics. Large enhancements of CO and O_3 were accompanied by no enhancement in aerosol-associated ionic species. The second plume on flight 12 was first sampled at about 0045 at an altitude near 6.5 km (Figure 4). The large increase of the CO mixing ratio in this case was accompanied by a relatively small O_3 increase, but the mixing ratio of NH_4^+ in our first sample (529 pptv) was the highest measured at any time during PEM-Tropics. The SO_4^{2-} mixing ratio in this sample (287 pptv) was also the highest free tropospheric value that we measured (Figures 1, 2, and 4). The second sample collected during this leg showed small decreases in the mixing ratios of CO, SO_4^{2-} , and NH_4^+ , but the levels of the aerosol-associated species were still greatly enhanced compared to the bulk of our free troposphere samples. We ascended above the plume for about 40 min, then reentered it at ≈ 0200 . Our first sample interval during the 6 km level leg again revealed elevated mixing ratios of CO, SO_4^{2-} , and NH_4^+ , with only a small enhancement in O_3 . The mixing ratios of the ionic species in this second plume encounter were only about 65% of those seen earlier, but were still more than 1.5-fold higher than any other samples collected between 2 and 8 km during PEM-Tropics (Figures 1, 2, and 4). During the second sample of this level flight leg the DC-8 passed out of the plume.

The anomalous plume in the 30° – 40°S latitude band on flight 12 was the only case when any of the aerosol-associated ionic species

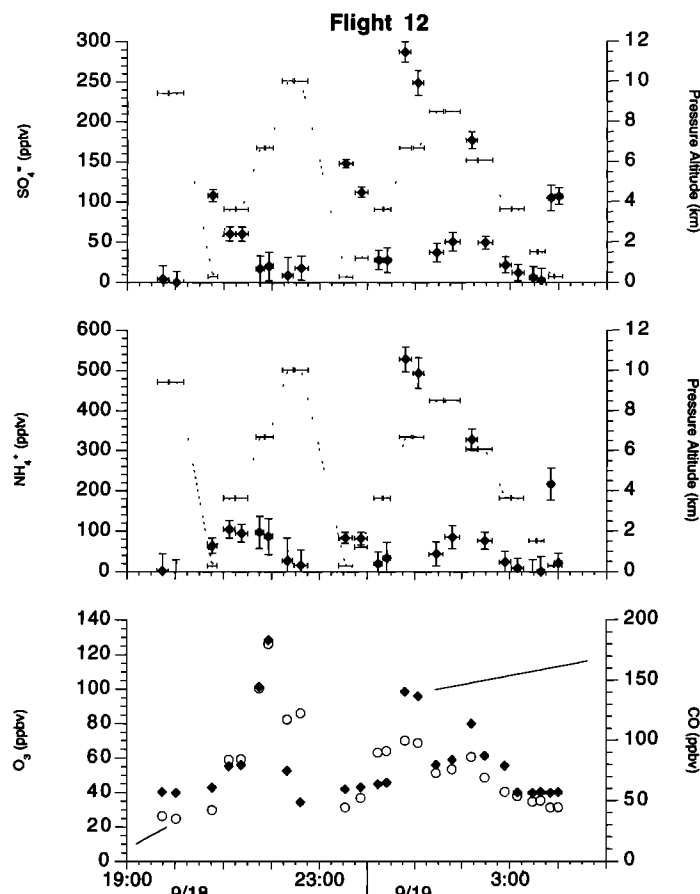


Figure 4. Time series of the mixing ratios of aerosol-associated SO_4^{2-} and NH_4^+ (solid diamonds), with average mixing ratios of O_3 (solid diamonds) and CO (open circles) for each aerosol collection interval, during the transit from Tahiti to New Zealand (flight 12). The dotted lines in the panels with aerosol composition indicate the altitude profile flown. Horizontal error bars define the integration period for each filter sample, and the vertical bars reflect uncertainty in the mixing ratios of the aerosol-associated ions.

increased with the gaseous tracers of combustion. The elevated mixing ratios of SO_4^- and NH_4^+ in this singular plume suggest that large quantities of soluble aerosols and their precursors were removed from all of the other plumes at some point during transport to the South Pacific. Scavenging by precipitation seems the most likely process, with several lines of evidence suggesting that removal of primary aerosols and gaseous precursors of soluble aerosols occurred far upwind of the PEM-Tropics study region, perhaps in deep wet convective systems that lofted the fire emissions into the free troposphere. We cannot rule out precipitation scavenging at later times during transport on the basis of the depressed mixing ratios of aerosol-associated species alone, but the very high mixing ratios of nitric and carboxylic acids in many of the plumes [Talbot *et al.*, this issue] require at least several days between any cleansing by scavenging and interception by the DC-8. Similarly, the elevated ^7Be activities throughout the free troposphere over the South Pacific (Figure 3) would not have survived recent or frequent scavenging by rain, as we observed during the PEM-West campaigns [Dibb *et al.*, 1996, 1997]. Furthermore, every plume-impacted aerosol sample that we have analyzed for ^{210}Pb so far contained ^{210}Pb activities that were 2 to 4 times higher than other free troposphere samples on the same flights. This is similar to our findings during the PEM-West missions, where vertical pumping of ^{222}Rn in deep wet convection (that scavenged soluble aerosols and gases) resulted in ^{210}Pb being the only aerosol-associated species that was enhanced in free tropospheric air concurrent with elevated concentrations of insoluble anthropogenic trace gases from the boundary layer [Dibb *et al.*, 1996, 1997].

4.1.2. Sulfur cycle. Emission of S gases (principally dimethylsulfide [e.g., Bates *et al.*, 1992a; Spiro *et al.*, 1992]) from the ocean and their conversion into the S-bearing aerosol species non-sea-salt (nss) SO_4^- and methylsulfonate (MSA) are topics of great current interest due to the possible importance of direct and

indirect radiative effects of new particles formed in remote oceanic regions [e.g. Charlson *et al.*, 1987]. Davis *et al.* [this issue] and Clarke *et al.* [1997] discuss the results of several flights by the P-3B during PEM-Tropics that were designed to investigate the sulfur budget and extent of new particle production in the equatorial South Pacific. Our sampling from the DC-8 was in more of a survey mode, covering large distances but not allowing much insight into processes, especially those occurring in the marine boundary layer. However, the distributions of nss SO_4^- and MSA in the free troposphere over the Pacific that we obtained appear to be unique.

The vertical profiles of MSA and nss SO_4^- (calculated with Mg^{2+} as the sea-salt indicator) show decreasing trends with altitude up to about 10 km (Figure 5), consistent with surface emissions of DMS as a major source of both species. The three samples with elevated nss SO_4^- are from the anomalous plume on flight 12 discussed above. On the other hand, DMS is the only known source of MSA, so the elevated MSA mixing ratios above 10 km must reflect pumping of MSA, or, as we will show is more likely, DMS from the marine boundary layer into the upper troposphere. Mixing ratios of nss SO_4^- increased little, if at all, above 10 km, so the molar ratio $\text{MSA}/\text{nss SO}_4^-$ (R) also increased dramatically above 10 km (Figure 5).

Examining these data as a function of latitude provides important insight into the large-scale distribution of biogenic sulfur aerosols over the Pacific (Figure 6). Below 2 km the MSA mixing ratio near 45°N was 3-4 times higher than in all other regions, but the nss SO_4^- mixing ratios in these samples were also relatively high, yielding values for R near 0.1 (Figure 6a). Between roughly 20°N and 35°S the mixing ratios of MSA and nss SO_4^- varied considerably, but most values of R were < 0.05 . The mixing ratios and variability of both species tended to decrease south of 35°S , with nss SO_4^- mixing ratios dropping more and faster than those of MSA. As a result, R increased with latitude (Figure 6a). (Our data

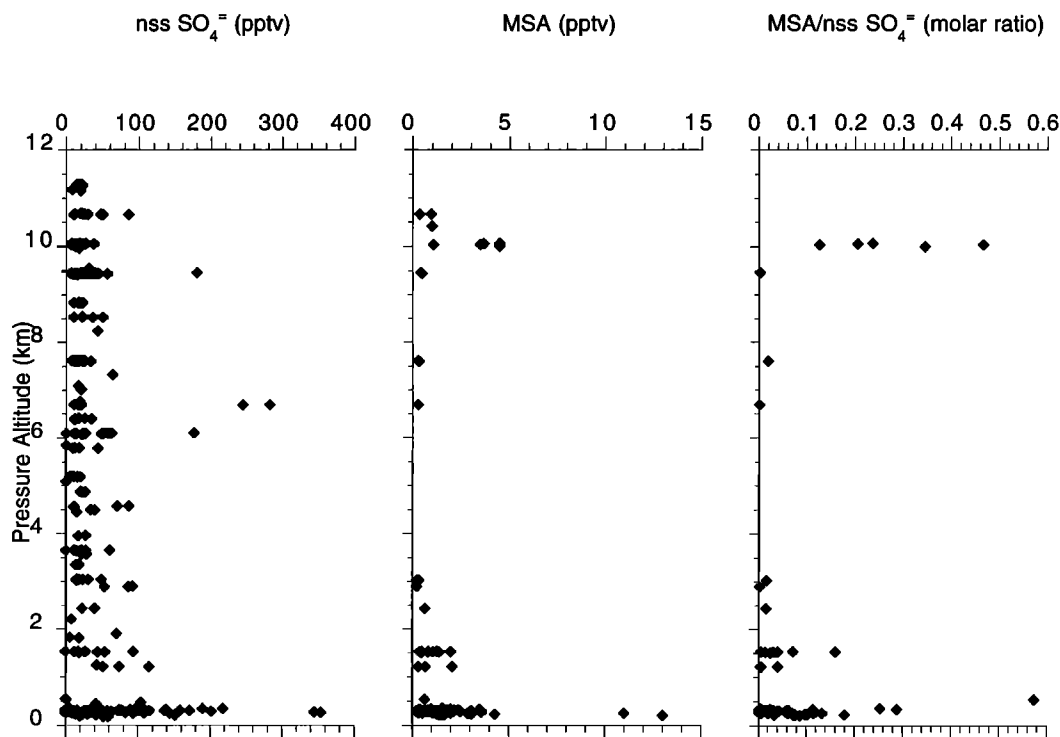


Figure 5. Altitude distributions of nss SO_4^- (calculated using Mg^{2+} as the sea-salt indicator), aerosol-associated MSA, and their molar ratio. Samples from all regions are combined.

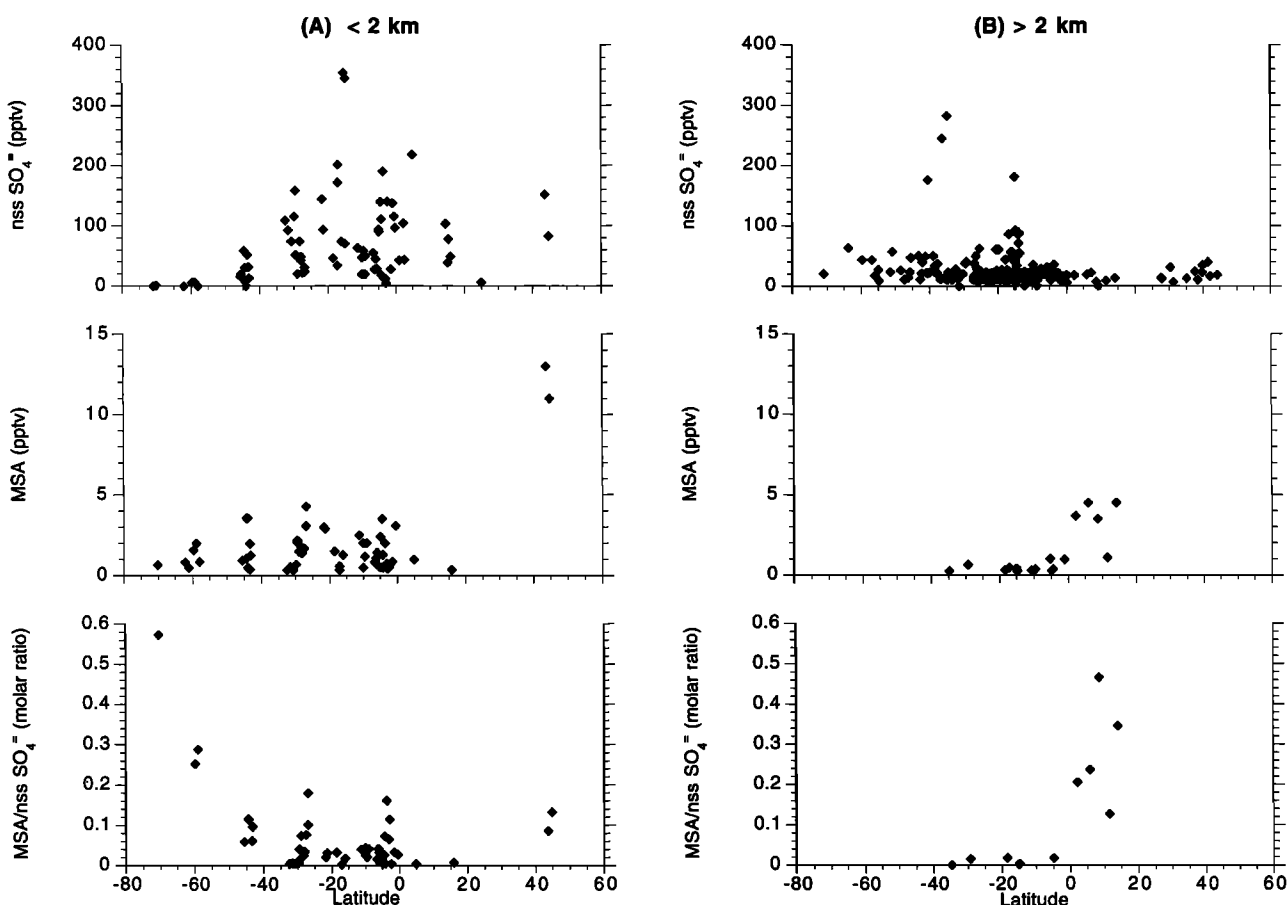


Figure 6. Distributions of nss SO_4^- , MSA, and their molar ratio as a function of latitude during PEM-Tropics. Data are separated into two altitude bins; (a) the marine boundary layer below 2 km and (b) the free troposphere above 2 km, but samples from all geographic regions are combined.

set provides only a hint of an increase in R with increasing latitude north of the equator due to the small number of samples, but the mid to high-latitude samples in the southern hemisphere reveal a steady increase from about 0.1 at 45°S to nearly 0.6 at 70°S . The increasing trend of R with latitude in the PEM-Tropics data set is similar to a profile measured by *Bates et al.* [1992a] on a cruise in the eastern Pacific (between 105° and 110°W and 20°N to 60°S) in February and March 1989. Boundary layer values of R in the submicron fraction of the aerosol on this cruise were less than 0.01 between 10°N and 10°S , increased to 0.05 from 10° – 30°S , and then rapidly increased to 0.18 near 40°S and 0.32 at 58°S (compare to the lower panel of Figure 6a). These authors suggested that the relative increase of MSA at higher latitudes was consistent with laboratory studies [*Hynes et al.*, 1986; *Yin et al.*, 1990] that found MSA to be favored over SO_2 as the product of DMS oxidation as both temperature and light intensity decreased. In fact, high values of R found in low-altitude aerosol samples from the high latitudes of both hemispheres have been tentatively ascribed mainly to the temperature dependence of the DMS branching ratio [e.g., *Berresheim*, 1987; *Pszenny et al.*, 1989; *Burgermeister and Georgii*, 1991; *Bates et al.*, 1992a; *Li et al.*, 1993; *Berresheim et al.*, 1995].

It must be noted that several investigations have found large variations in R as a function of particle size. The presence of a much more pronounced supermicron mode for MSA than for nss SO_4^- results in higher values of R in the larger fractions of the

aerosol population. This effect has been observed most frequently in the tropical Pacific: *Quinn et al.* [1993] found R to increase from 0.01 in the submicron fraction to 0.02 when all stages of an impactor sample (0–4 micron range) collected at 22°N were composited, *Huebert et al.* [1993] found a similar increase ($R = 0.04$ for $D_p < 1 \mu\text{m}$ compared to 0.07 in bulk (maximum diameter $10 \mu\text{m}$) during the equatorial Soviet-American Gas and Aerosol (SAGA) 3 cruise, while *Huebert et al.* [1996] reported an even larger increase between submicron and bulk values of R (0.016 to 0.053) during their 1994 sampling campaign on Christmas Island (2°N). In the tropical Atlantic the limited data do not provide a clear picture. *Andreae et al.* [1995] found R to increase from 0.049 to 0.066 when comparing submicron to bulk, while *Putaud et al.* [1993] did not see a significant supermicron mode of MSA, hence R varied little with particle size. In extratropical regions (but also closer to landmasses) any variations of R as a function of particle size have been quite small [*Saltzman et al.*, 1983, 1986a, b; *Pszenny et al.*, 1989].

The preceding suggests that comparison between our bulk aerosol samples and surface-based results must consider the size range collected in previous studies and whether our system is biased against the larger particles. In the tropics where the dependence of R on particle size is expected to be largest, our 20 boundary layer samples (Figure 6a) have a mean R of 0.043. The low (< 0.01) values reported by *Bates et al.* [1992a] are for fine ($< 0.6 \mu\text{m}$) particles, and we can estimate that the bulk value might be 2 to 3 times higher. *Quinn et al.* [1990] measured an average R of about 0.03 between 9°N and 7°S for fine

samples (1 μm cut), and bulk values would presumably be higher but probably by no more than a factor of 2. Our mean value is 75% of the average bulk value (0.053) reported by Huebert *et al.* [1996] from Christmas Island and 2.7 times higher than the submicron average (0.016) for these same samples. These comparisons suggest that our sampling system is efficiently passing a high fraction of the large aerosol particles present in the marine boundary layer (more precisely, it appears that any inlet losses we do experience are nearly proportionately impacting both fine and coarse fractions, and we assume that the passing efficiency for the submicron particles is high). Of course, such comparisons are based on short periods of observation at different times and places, so they cannot be considered a rigorous test of our inlet design and performance.

The obvious benefit of airborne sampling as a complement to surface-based campaigns is that distributions in the free troposphere can only be determined from an airborne platform. For the case of the biogenic S aerosols, the free troposphere is quite different than the marine boundary layer. The samples with high MSA and R values above 10 km (Figure 5) were all clustered near the ITCZ, which was centered near 10°N when the DC-8 crossed it in early September and then again in early October (Figure 6b). Convection in the ITCZ would appear to be the mechanism lofting marine boundary layer air into the upper troposphere. We hypothesize that when DMS is pumped into the upper troposphere, the cold temperatures favor production of MSA over SO_2 , leading to increased values of R. The lifetime of DMS in the tropical marine boundary layer is not very well constrained, but is likely to be of the order of several hours to no more than a few days [Huebert *et al.*, 1993, and references therein]. Given such short lifetimes of DMS in the boundary layer, finding significant mixing ratios of DMS in the free troposphere implies very frequent vertical transport events [e.g., Chatfield and Crutzen, 1984]. Mixing ratios of DMS above 6 km near 10°N ranged from 17–45 pptv (when averaged to aerosol sample integration times), compared to a 30–60 pptv range in the boundary layer in the same region (data not shown). The R values in the upper troposphere near the ITCZ are so high relative to those in the tropical boundary layer (in fact, compared to all boundary layer values between 20°N and 45°S), and the mixing ratios of nss SO_4^{2-} are so low (Figures 5 and 6), that it is likely that very little boundary layer aerosol is transported along with the DMS. We therefore suggest that wet convective events which efficiently scavenge the aerosols present in the marine boundary are the most important agents of vertical uplift transporting DMS into the tropical free troposphere.

It should also be noted that the biogenic S aerosols in the upper troposphere are more likely to be transported long distances than those that remain within the marine boundary layer. Our data thus suggest that interpreting R values measured in polar ice cores as a straightforward indication of the latitude from which an air mass carried water vapor and biogenic S to high latitudes [e.g., Legrand and Feniet-Saigne, 1991; Legrand *et al.*, 1991; Whung *et al.*, 1994] may be misleading. The well established latitudinal trend in R at low altitudes would suggest high-latitude origins for all of the upper troposphere samples between 0° and 20°N (Figure 6), yet it is quite clear that the biogenic S in these samples originated in the tropical or subtropical marine boundary layer.

4.2. Boundary Layer Distributions

4.2.1. Marine source of ammonia. The decreasing mixing ratios of NH_4^+ with increasing altitude in all regions sampled during PEM-Tropics (Figure 2) are consistent with a surface source. Quinn *et al.* [1990] and Clarke and Porter [1993] have presented evidence from recent cruises that significant amounts of NH_3 are emitted from the Pacific Ocean, particularly in equatorial regions. Our NH_4^+ data appear to reinforce these findings.

Mixing ratios of NH_4^+ in the marine boundary layer (<2 km) samples varied over a wide range in most latitude bands, though nearly all samples with elevated mixing ratios (>200 pptv) were collected within 20° of the equator (Figure 7). The tropical regions are also characterized by a more pronounced enhancement of boundary layer NH_4^+ mixing ratios relative to the overlying free troposphere. Similar trends were found in CH_3I , and to a lesser extent DMS, two trace gases known to be dominated by emission from the surface ocean [e.g., Singh *et al.*, 1983; Bates *et al.*, 1992b].

4.2.2. Coupling of the N and S cycles in the Pacific marine boundary layer. It has been suggested that most of the submicron sulfate aerosol in the Pacific boundary layer far from continental sources of NH_3 is present as H_2SO_4 [Yamato *et al.*, 1989; Yamato and Tanaka, 1994]. On the other hand, Quinn *et al.* [1990] reported $\text{NH}_4^+/\text{nss SO}_4^{2-}$ molar ratios in the range of 0.8 to 1.9 in tropical regions of the Pacific where they inferred significant emissions of NH_3 . Similarly, Clarke and Porter [1993] based their estimation of NH_3 fluxes from the equatorial Pacific on observations of decreased volatility of submicron aerosols due to neutralization of H_2SO_4 droplets to form NH_4HSO_4 and $(\text{NH}_4)_2\text{SO}_4$. Our results during PEM-Tropics indicate that H_2SO_4 did not constitute a major fraction of the boundary layer aerosol mass in any of the regions we sampled.

Scatterplots of NH_4^+ versus nss SO_4^{2-} reveal that only a few of our bulk aerosol samples were more acidic than would be consistent with NH_4HSO_4 as the dominant form of sulfate (Figure 8). In fact, more than 40% of all samples collected in the southern hemisphere, and all of those from east of 120°W, had more NH_4^+ than would be required to completely neutralize SO_4^{2-} to $(\text{NH}_4)_2\text{SO}_4$. If we assume that all measured aerosol NO_3^- reacted with NH_4^+ to form NH_4NO_3 after nss SO_4^{2-} was depleted, we are still left with "excess" NH_4^+ in more than 25% of the southern hemisphere samples and 9/11 samples collected east of 120°W. This is an unexpected result that is not readily explained, so we must consider whether it is real or an artifact caused by some aspect of our sampling, chemical analysis,

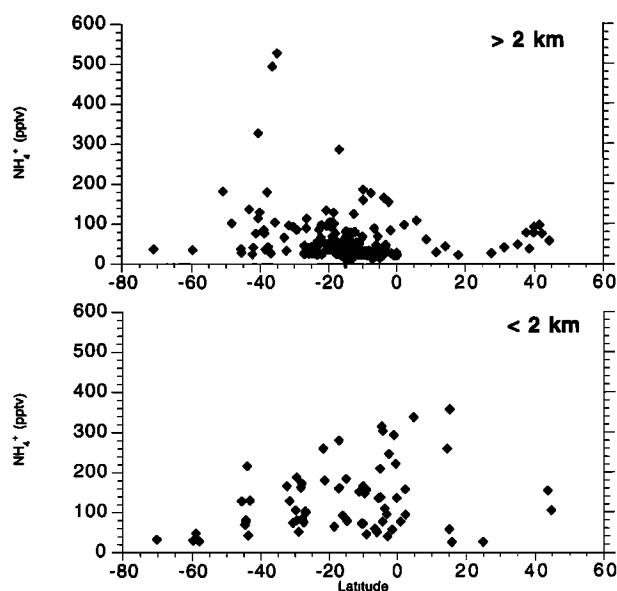


Figure 7. Mixing ratios of NH_4^+ as a function of latitude. The upper panel includes all samples collected above 2 km pressure altitude, and the lower panel includes those collected below 2 km.

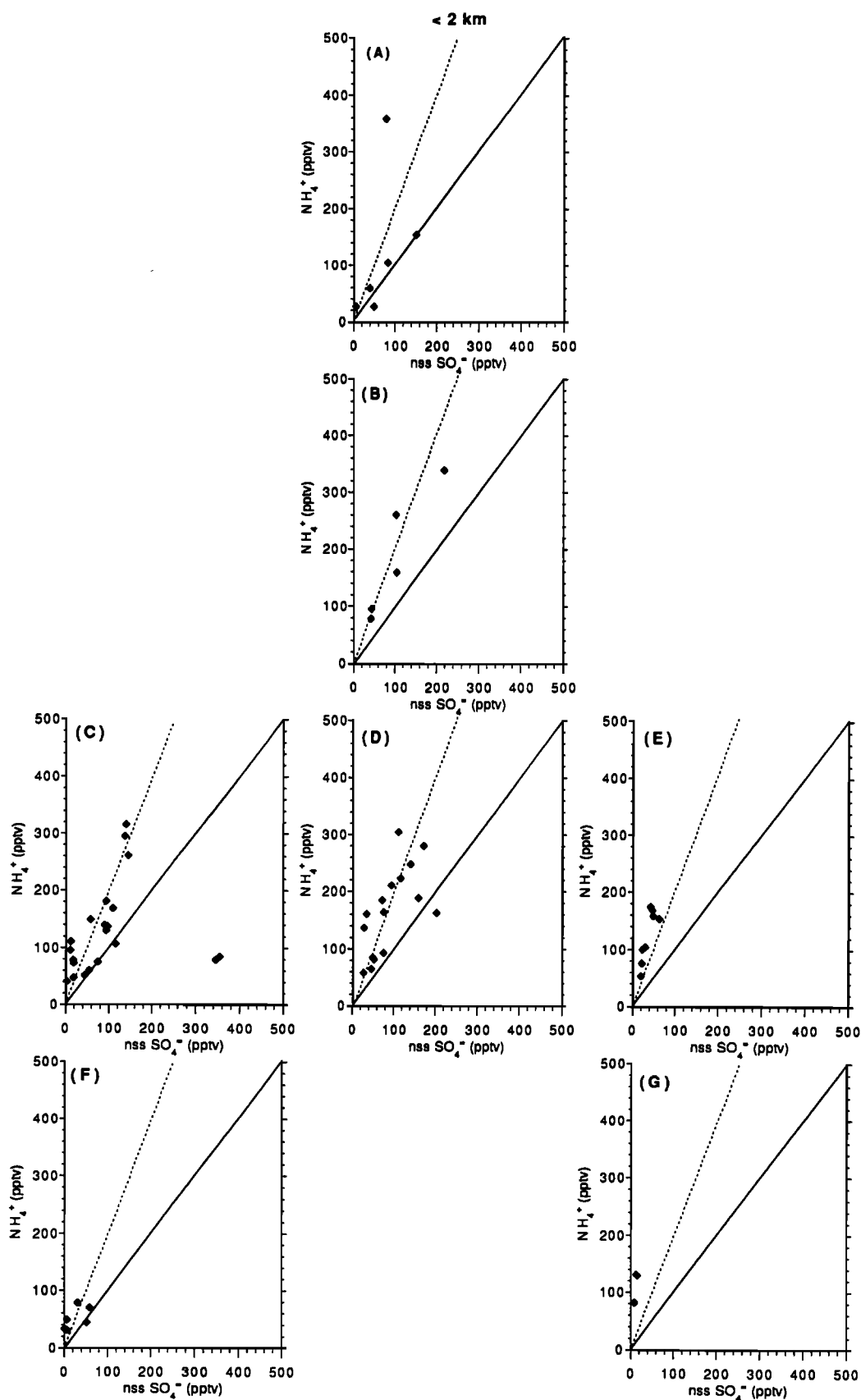


Figure 8. Scatterplots of NH_4^+ against nss SO_4^- . The solid line in each panel is the 1:1 ratio corresponding to NH_4HSO_4 , and the dotted line is the 2:1 ratio corresponding to $(\text{NH}_4)_2\text{SO}_4$. Panels reflect the same geographic regions as in Figures 1-3.

or data reduction. It should be noted that, although we have flown numerous GTE missions over the oceans, PEM-Tropics is the first case where our aerosol NH_4^+ measurements have suggested a dominant marine source of NH_3 .

It is possible that, despite our efforts to minimize exposure of collected aerosols to air inside the DC-8 cabin, some fraction of the measured NH_4^+ is an artifact of NH_3 reacting with acidic aerosols on the filters [e.g., Hayes *et al.*, 1980]. However, the samples collected in the marine boundary are so heavily loaded with sea salt that there is not likely to be much free acidity on the filters to drive such postcollection acid/base reactions. Furthermore, this type of artifact would not seem capable of pushing the $\text{NH}_4^+/\text{nss SO}_4^-$ ratio above the complete neutralization value of 2. It is also possible that the samples picked up NH_3 diffusing through the walls of the polyethylene bottles during transit back to our laboratory, but the NH_4^+ concentrations in PEM-Tropics blanks were not elevated compared to any other field program in which we have participated.

The magnitude of the excess NH_4^+ in most of the samples that have "too much" NH_4^+ is well above our analytical uncertainty. Sample volumes in the boundary layer were generally two- to three-fold greater than the mission mean of 4.2 m^{-3} STP, reducing uncertainty from blank subtraction to levels of the order of 5 pptv total SO_4^- and 10 pptv NH_4^+ . Similarly, while it is possible that our sampling system is oversampling large particles in the boundary layer, which would lead to overestimation of the sea-salt fraction of SO_4^- and increase the $\text{NH}_4^+/\text{nss SO}_4^-$ ratio, our successful reproduction of the latitudinal profile of $\text{MSA}/\text{nss SO}_4^-$ suggests little or no such bias. (Note that losses of large particles in the inlet would be more likely than oversampling.) We could also be overestimating sea-salt SO_4^- by adopting the standard assumption that there is no fractionation between Mg^{2+} and SO_4^- during formation of sea-salt aerosols. This assumption has been shown to be invalid for aerosols and snow in coastal regions of Antarctica where the standard calculation yields substantially negative estimates of nss SO_4^- during winter (i.e., a modified sea-salt aerosol that has much less SO_4^- than expected from seawater composition is prevalent in this region) [Wagenbach *et al.*, 1988; Gjessing, 1989; Mulvaney *et al.*, 1992; Minikin *et al.*, 1994]. However, we are not aware of similar findings at lower latitudes. In any case, even if we make the extreme assumption that all of the measured SO_4^- is nss SO_4^- available to react with NH_3 , we still find that NH_4^+ is present in excess in 10/66 southern hemisphere samples, with most of these from the western (five samples) and central (three samples) 0° - 35°S bins.

In summary, it appears that the presence of excess NH_4^+ was a real characteristic of some of the regions sampled during PEM-Tropics, though the frequency of such aerosols may be less than suggested by the number of points above the 2:1 lines in Figure 8. We speculate that dissolution of NH_3 into hydrated sea-salt aerosols could account for the excess NH_4^+ . In this case the solubility of NH_3 in the aqueous phase, rather than the presence of an acidic counter anion, would determine the final concentration of NH_4^+ in the extract of the filter. It is not possible to confirm this hypothesis from the PEM-Tropics data set, nor can we be certain that the excess NH_4^+ goes into the aerosol phase in the ambient marine boundary layer rather than on the filters during (or after) sample collection. It should be possible to test this hypothesis through chemical characterization of size-fractionated aerosol samples from the South Pacific boundary layer, since NH_3 dissolving into wet sea-salt aerosols would be found in the large particle mode (though it would still be difficult to discriminate between NH_3 uptake in the ambient aerosol versus artifact uptake by aerosols concentrated onto

a filter during sampling). We note that Quinn *et al.* [1993] and Andreae *et al.* [1995] found no evidence for supermicron NH_4^+ in samples collected in the North Pacific and South Atlantic, respectively, but the $\text{NH}_4^+/\text{nss SO}_4^-$ ratios in these regions were generally ≤ 1.0 , hence excess NH_3 was probably not available.

5. Conclusions

The extensive influence of biomass burning plumes in the free troposphere over the South Pacific was an unexpected highlight of the PEM-Tropics airborne sampling campaign. With only a single exception, these plumes did not carry enhanced levels of soluble aerosols into the region, as might have been expected based on previous characterizations of such plumes around the world. Precipitation scavenging apparently depressed the concentrations of soluble ions and their gaseous precursors. High ^7Be activities throughout the South Pacific troposphere imply that this cleansing must have occurred early in the plumes' history rather than shortly before they were intercepted by the DC-8. Elevated mixing ratios of nitric and carboxylic acids in most of the plumes [Talbot *et al.*, this issue] support the inference based on ^7Be , as these gases would also have been scavenged in recent precipitation events.

Mixing ratios of DMS up to 45 pptv, aerosol-associated MSA near 5 pptv, and values of the $\text{MSA}/\text{nss SO}_4^-$ molar ratio in the range of 0.2-0.5 near 10 km altitude between the equator and 10°N must reflect frequent and deep vertical mixing by wet convection in the ITCZ. The high values of the $\text{MSA}/\text{nss SO}_4^-$ ratio in this region are particularly noteworthy, as the latitudinal profile developed through surface-based sampling displays a tropical minimum (≤ 0.05) and increases toward higher latitudes. The values we measured at altitude in the tropics would not be expected in surface air until latitudes greater than about 60° were reached.

Decreasing mixing ratios of NH_4^+ with increasing altitude throughout the PEM-Tropics study area suggest that emission of NH_3 from the ocean is an important source for remote marine air. The latitude distribution of NH_4^+ in the boundary layer ($< 2 \text{ km}$) shows that the highest mixing ratios were found in the tropics, consistent with recent shipboard sampling campaigns that suggested relatively strong emissions of NH_3 from the equatorial Pacific [Quinn *et al.*, 1990; Clarke and Porter, 1993].

Our observation of excess NH_4^+ in many PEM-Tropics boundary layer samples is somewhat problematic. We cannot entirely rule out the possibility that these data are artifacts of sampling and/or data processing, but feel that they are indicating a real feature of the boundary layer aerosol in some regions of the South Pacific. If so, the details of incorporation of NH_3 into the aerosol phase in the marine boundary layer merit additional attention.

Acknowledgments. The efforts of the Ames DC-8 flight and ground crews that made PEM-Tropics a success are greatly appreciated. We would also like to thank the two anonymous reviewers for their insightful comments that greatly improved the clarity of this paper. This research was supported by the NASA Global Tropospheric Chemistry Program.

References

- Andreae, M. O., W. Elbert, and S. J. de Mora, Biogenic sulfur emissions and aerosols over the tropical South Atlantic, 3, Atmospheric dimethylsulfide, aerosols, and cloud condensation nuclei, *J. Geophys. Res.*, **100**, 11,335-11,356, 1995.
- Ayers, G. P., J. P. Ivey, and H. S. Goodman, Sulfate methanesulfonate at Cape Grim, Tasmania, *J. Atmos. Chem.*, **4**, 173-185, 1986.
- Bates, T. S., A. D. Clarke, V. N. Kapustin, J. E. Johnson, and R. J. Charlson, Oceanic dimethylsulfide and marine aerosol: Difficulties

- associated with assessing their covariance, *Global Biogeochem. Cycles*, **3**, 299-304, 1989.
- Bates, T. S., J. A. Calhoun, and P. K. Quinn, Variations in the methanesulfonate to sulfate molar ratio in submicrometer marine aerosol particles over the South Pacific Ocean, *J. Geophys. Res.*, **97**, 9859-9865, 1992a.
- Bates, T. S., B. K. Lamb, A. Guenther, J. Dignon, and R. E. Stoiber, Sulfur emission to the atmosphere from natural sources, *J. Atmos. Chem.*, **14**, 315-337, 1992b.
- Berresheim, H., Biogenic sulfur emissions from the subantarctic and Antarctic oceans, *J. Geophys. Res.*, **92**, 13,245-13,262, 1987.
- Berresheim, H., P. H. Wine, and D. D. Davis, Sulfur in the atmosphere, in *Composition, Chemistry, and Climate of the Atmosphere*, edited by H. B. Singh, 251-307, Van Nostrand Reinhold, New York, 1995.
- Burgermeister, S., and H. W. Georgii, Distribution of methanesulfonate, nss sulfate and dimethylsulfide over the Atlantic and the North Sea, *Atmos. Environ., Part A*, **25**, 587-595, 1991.
- Charlson, R. J., J. E. Lovelock, M. O. Andreae, and S. G. Warren, Oceanic phytoplankton, atmospheric sulphur, cloud albedo and climate: A geophysical feedback, *Nature*, **326**, 655-661, 1987.
- Chatfield, R. B., and P. J. Crutzen, Sulfur dioxide in remote oceanic air: Cloud transport of reactive precursors, *J. Geophys. Res.*, **89**, 7111-7132, 1984.
- Clarke, A. D., and J. N. Porter, Pacific marine aerosol, 2, Equatorial gradients in chlorophyll, ammonium, and excess sulfate during SAGA 3, *J. Geophys. Res.*, **98**, 16,997-17,010, 1993.
- Clarke, A. D., K. G. Moore, Z. L. Varner, and F. Eisle, Three regimes for new particle production in the Pacific troposphere: Cumulus outflow, aged pollution, and the equatorial boundary layer (abstract), *Eos Trans. AGU*, **78(46)**, F98, 1997.
- Davis, D. D., et al., DMS oxidation in the equatorial Pacific: Comparison of model simulations with field observations for DMS, SO₂, H₂SO₄(g), MSA(g), MS, and NSS, *J. Geophys. Res.*, this issue.
- Dibb, J. E., R. W. Talbot, K. I. Klemm, G. L. Gregory, H. B. Singh, J. D. Bradshaw, and S. T. Sandholm, Asian influence over the western North Pacific during the fall season: Inferences from lead 210, soluble ionic species, and ozone, *J. Geophys. Res.*, **101**, 1779-1792, 1996.
- Dibb, J. E., R. W. Talbot, B. L. Lefter, E. Scheuer, G. L. Gregory, E. V. Browell, J. D. Bradshaw, S. T. Sandholm, and H. B. Singh, Distributions of beryllium-7, lead-210, and soluble aerosol-associated ionic species over the western Pacific: PEM-West B, February-March, 1994, *J. Geophys. Res.*, **102**, 28,287-28,302, 1997.
- Fuelberg, H., et al., A meteorological overview of the PEM-Tropics period, *J. Geophys. Res.*, this issue.
- Gjessing, Y. T., Excess and deficit of sulfate in polar snow, *Atmos. Environ.*, **18**, 825-830, 1989.
- Gregory, G. L., et al., Chemical characteristics of Pacific tropospheric air in the region of the ITCZ and SPCZ, *J. Geophys. Res.*, this issue.
- Hayes, D., K. Snetsinger, G. Ferry, V. Overbeck, and N. Farlow, Reactivity of stratospheric aerosol to small amounts of ammonia in the laboratory environment, *Geophys. Res. Lett.*, **7**, 974-976, 1980.
- Hoell, J. M., Jr., et al., Pacific Exploratory Mission in the tropical Pacific: PEM-Tropics A, August-September 1996, *J. Geophys. Res.*, this issue.
- Huebert, B. J., G. Lee, and W. L. Warren, Airborne aerosol inlet passing efficiency measurement, *J. Geophys. Res.*, **95**, 16,369-16,381, 1990.
- Huebert, B. J., S. Howell, P. Laj, J. E. Johnson, T. S. Bates, P. K. Quinn, V. Yegorov, A. D. Clarke, and J. N. Porter, Observations of the atmospheric sulfur cycle on SAGA 3, *J. Geophys. Res.*, **98**, 16,985-16,995, 1993.
- Huebert, B. J., D. J. Wylie, L. Zhuang, and J. A. Heath, Production and loss of methanesulfonate and non-sea-salt sulfate in the equatorial Pacific marine boundary layer, *Geophys. Res. Lett.*, **23**, 737-740, 1996.
- Hynes, A. J., P. H. Wine, and D. H. Semmes, Kinetics and mechanisms of OH reactions with organic sulfides, *J. Phys. Chem.*, **90**, 4148-4156, 1986.
- Legrand, M., and C. Feniet-Saigne, Methanesulfonic acid in South Pole snow layers: A record of strong El Niño?, *Geophys. Res. Lett.*, **18**, 187-190, 1991.
- Legrand, M., C. Feniet-Saigne, E. S. Saltzman, C. Germain, N. I. Barkov, and V. N. Petrov, Ice core record of oceanic emissions of dimethylsulphide during the last climatic cycle, *Science*, **350**, 144-146, 1991.
- Li, S.-M., L. A. Barrie, R. W. Talbot, R. C. Harriss, C. I. Davidson, and J.-L. Jaffrezo, Seasonal and geographic variations of methanesulfonic acid in the Arctic troposphere, *Atmos. Environ., Part A*, **27**, 3011-3024, 1993.
- Minikin, A., D. Wagenbach, W. Graf, and J. Kipfstuhl, Spatial and seasonal variations of the snow chemistry at the central Filchner-Ronne Ice Shelf, *Ann. Glaciol.*, **20**, 283-290, 1994.
- Mulvaney, R., E. C. Pasteur, and D. A. Peel, The ratio of MSA to non-sea-salt sulfate in Antarctic Peninsula ice cores, *Tellus, Ser. B*, **44**, 295-303, 1992.
- Porter, J. N., A. D. Clarke, G. Ferry, and R. F. Pueschel, Aircraft studies of size-dependent aerosol sampling through inlets, *J. Geophys. Res.*, **97**, 3815-3824, 1992.
- Pszenny, A. A. P., A. J. Castelle, J. N. Galloway, and R. A. Duce, A study of the sulfur cycle in the Antarctic marine boundary layer, *J. Geophys. Res.*, **94**, 9818-9830, 1989.
- Putaud, J.-P., S. Belviso, B. C. Nguyen, and N. Mihalopoulos, Dimethylsulfide, aerosols, and condensation nuclei over the tropical northeastern Atlantic Ocean, *J. Geophys. Res.*, **98**, 14,863-14,871, 1993.
- Quinn, P. K., T. S. Bates, J. E. Johnson, D. S. Covert, and R. J. Charlson, Interactions between the sulfur and reduced nitrogen cycles over the central Pacific Ocean, *J. Geophys. Res.*, **95**, 16,405-16,416, 1990.
- Quinn, P. K., D. S. Covert, T. S. Bates, V. N. Kapustin, D. C. Ramsey-Bell, and L. M. McInnes, Dimethylsulfide/cloud condensation nuclei/climate system: Relevant size-resolved measurements of the chemical and physical properties of atmospheric aerosol particles, *J. Geophys. Res.*, **98**, 10,411-10,427, 1993.
- Raemdonck, H., W. Maenhaut, and M. O. Andreae, Chemistry of marine aerosol over the tropical and equatorial Pacific, *J. Geophys. Res.*, **91**, 8623-8636, 1986.
- Saltzman, E. S., D. L. Savoie, R. G. Zika, and J. M. Prospero, Methane sulfonic acid in the marine atmosphere, *J. Geophys. Res.*, **88**, 10,897-10,902, 1983.
- Saltzman, E. S., D. L. Savoie, J. M. Prospero, and R. G. Zika, Methanesulfonic acid and non-sea-salt sulfate in Pacific air: Regional and seasonal variations, *J. Atmos. Chem.*, **4**, 227-240, 1986a.
- Saltzman, E. S., D. L. Savoie, J. M. Prospero, and R. G. Zika, Elevated atmospheric sulfur levels off the Peruvian coast, *J. Geophys. Res.*, **91**, 7913-7918, 1986b.
- Savoie, D. L., and J. M. Prospero, Comparison of oceanic and continental sources of non-seasalt sulfate over the Pacific Ocean, *Nature*, **339**, 685-687, 1989.
- Singh, H. B., L. J. Salas, and R. E. Stiles, Methyl halides in and over the eastern Pacific (40°N-32°S), *J. Geophys. Res.*, **88**, 3684-3690, 1983.
- Spiro, P. A., D. J. Jacob, and J. A. Logan, Global inventory of sulfur emissions with a 1° x 1° resolution, *J. Geophys. Res.*, **97**, 6023-6036, 1992.
- Talbot, R. W., J. E. Dibb, E. M. Scheuer, D. R. Blake, N. J. Blake, G. L. Gregory, G. W. Sachse, J. D. Bradshaw, S. T. Sandholm, and H. B. Singh, Influence of biomass combustion emissions on the distribution of acidic trace gases over the southern Pacific basin during austral springtime, *J. Geophys. Res.*, this issue.
- Wagenbach, D., U. Görlach, K. Moser, and K.O. Münnich, Coastal Antarctic aerosol: The seasonal pattern of its chemical composition and abundance, *Tellus, Ser. B*, **40**, 426-436, 1988.
- Whung, P.-Y., E. S. Saltzman, M. J. Spencer, P. A. Mayewski, and N. Gundestrup, Two-hundred-year record of biogenic sulfur in a south Greenland ice core (20D), *J. Geophys. Res.*, **99**, 1147-1156, 1994.
- Yamato, M., and H. Tanaka, Aircraft observations of aerosols in the free marine troposphere over the North Pacific Ocean: Particle chemistry in relation to air mass origin, *J. Geophys. Res.*, **99**, 5353-5377, 1994.
- Yamato, M., Y. Iwasaka, G.-W. Qian, A. Ono, T. Yamanouchi, and A. Sumi, Sulfuric acid particles and their neutralization by ammonia in the marine atmosphere: Measurements during cruise from Japan to Antarctica, *Proc. NIPR Symp. Polar Meteorol. Glaciol.*, **2**, 29-40, 1989.
- Yin, F., D. Grosjean, and J. H. Seinfeld, Photooxidation of dimethyl sulfide and dimethyl disulfide, I, Mechanism development, *J. Atmos. Chem.*, **11**, 309-364, 1990.

D. R. Blake and N. J. Blake, Department of Chemistry, University of California, Irvine, CA 92717.

J. E. Dibb (corresponding author), E. M. Scheuer, and R. W. Talbot, Institute for the Study of Earth, Oceans, and Space, University of New Hampshire, Durham, NH 03824. (e-mail: jack.dibb@unh.edu)

G. L. Gregory and G. W. Sachse, NASA Langley Research Center, Hampton, VA 23681.

D. C. Thornton, Department of Chemistry, Drexel University, Philadelphia, PA 19104.

(Received January 12, 1998; revised August 28, 1998; accepted August 31, 1998.)